

## Effects of noise in different approaches for the statistics of polariton condensates

Davide Sarchi, Paolo Schwendimann, and Antonio Quattropani

*Institute of Theoretical Physics, École Polytechnique Fédérale de Lausanne, CH 1015 Lausanne-EPFL, Switzerland*

(Received 22 May 2008; revised manuscript received 16 July 2008; published 14 August 2008)

The second-order correlation function of the polariton condensate is calculated within two different approaches. Both approaches qualitatively reproduce the deviations from the full coherence of the second-order correlation function that have been observed in the experiments. However, a quantitative difference in the magnitude of the predicted deviations is found. This difference originates in the modeling of the polariton dynamics in the two approaches.

DOI: [10.1103/PhysRevB.78.073404](https://doi.org/10.1103/PhysRevB.78.073404)

PACS number(s): 71.35.Lk, 71.36.+c, 71.55.Gs, 73.21.Fg

As it is well known, polaritons in semiconductor microcavities are excellent candidates for observing condensation in solid-state systems due to their small mass ( $m/m_e = 7 \cdot 10^{-5}$  in CdTe). The experimental value of the transition temperature  $T_c$  ranges between 5 and 80 K<sup>1-3</sup>) and is ten orders of magnitude larger than in the case of atomic Bose-Einstein condensation. However, polariton condensation has to happen out of thermal equilibrium because it results from a balance between a pump mechanism and the losses that are responsible for the finite lifetime of the polaritons. Since the system in this configuration is an open system, it is expected that noise will play an important role in the characterization of the polariton condensate. The investigation of the role of noise in the condensation process has raised some interest once the experimental evidence of polariton condensation has been obtained.<sup>1-4</sup> In particular, noise effects in the polariton condensate have been experimentally demonstrated in Refs. 5-7 through the measurement of the second-order polariton correlation function  $g^{(2)}(0)$ . This quantity shows deviations from full coherence characterized by  $g^{(2)}(0) = 1$ . These deviations are interpreted as a signature of noise due to scattering processes between the condensate and the polariton excited modes. The behavior outlined above has been qualitatively reproduced in a recent theoretical paper<sup>8</sup> that deals with the statistical properties of the polariton condensate in the mode with  $q=0$ . The model considered in Ref. 8 takes advantage of the presence of a bottleneck in the exciton polariton dispersion.<sup>9</sup> It is assumed that the polaritons whose energies lay in the bottleneck region act as a reservoir, while polaritons whose energies lay below the bottleneck participate to the condensation dynamics. In particular it is shown that the nonresonant scattering processes between the polariton mode with  $q=0$  and the ones with  $\mathbf{q} \neq 0$  are responsible for the deviations from the fully coherent statistics observed in the experiments.<sup>5</sup> In the spirit of quantum optics,<sup>10</sup> we denote as noise the contribution of nonresonant scattering. The population density and the effective temperature of the reservoir in this approach are self-consistently determined within a generalization of the approach presented in Ref. 11. The statistics of the condensate is evaluated within the master-equation formalism. The injection and dissipation rates that appear in the master equation originate both from resonant and nonresonant scattering processes and depend on the populations of the polaritons with  $\mathbf{q} \neq 0$ . These populations depend in turn on the modeling of the reservoir. Therefore, we have to show that the deviations from full coherence

that are found in Ref. 8 are not an artifact related to the particular choice of the reservoir.

In the present Brief Report we discuss this last point by comparing the results from Ref. 8 with the ones obtained by fully describing the dynamics of the polaritons with  $\mathbf{q} \neq 0$  in a mean-field approximation, generalizing the approaches discussed in Refs. 12 and 13. The different polariton dynamics considered in the present Brief Report are reservoir-based approach schematically presented in Fig. 1.

The main difference between the two approaches consists in the fact that in the reservoir-based approach,<sup>8</sup> the populations of the polaritons in the bottleneck are described by a quasithermal equilibrium state whose effective temperature and particle density are consistently determined. The pump enters through the equations determining the stationary state of the reservoir. In the mean-field approach the dynamics of the modes with  $\mathbf{q} \neq 0$  is described by the equations

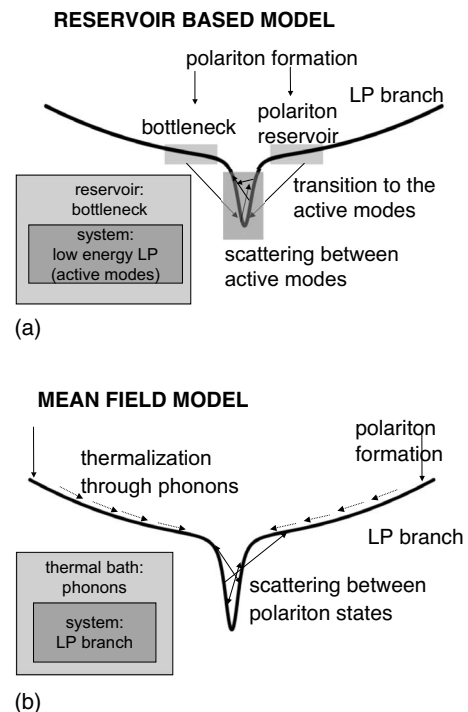


FIG. 1. Sketch of the polariton dynamics. (a) Reservoir-based model. (b) Mean-field model.

$$\begin{aligned} \hbar \frac{dN_{\mathbf{q}}}{dt} = & -2(\gamma_{\mathbf{q}} + \Gamma_{\mathbf{q},\text{TOT}} - \Delta_{\mathbf{q},\text{TOT}})N_{\mathbf{q}} + 2\Delta_{\mathbf{q},\text{TOT}} \\ & + W_{0,\mathbf{q},-\mathbf{q}}^2 \text{Re} \left\{ \frac{2N_0^2(N_{\mathbf{q}} + N_{-\mathbf{q}} + 1)}{[i\hbar(\omega_0 - \omega_{\mathbf{q}}) + \Sigma_{\text{TOT}} + \gamma_{\mathbf{q}}]} \right. \\ & \left. - \frac{2(2N_0 + 1)N_{\mathbf{q}}N_{-\mathbf{q}}}{[i\hbar(\omega_0 - \omega_{\mathbf{q}}) + \Sigma_{\text{TOT}} + \gamma_{\mathbf{q}}]} \right\} + F_{\mathbf{q}} \end{aligned} \quad (1a)$$

with

$$\Sigma_{\text{TOT}} = \gamma_0 + \Gamma_{0,\text{TOT}} - \Delta_{0,\text{TOT}}. \quad (1b)$$

In Eq. (1a),  $N_{\mathbf{q}} = \langle P_{\mathbf{q}}^\dagger P_{\mathbf{q}} \rangle$  is the polariton population in the  $\mathbf{q}$  state,  $\gamma_{\mathbf{q}}$  is the radiative linewidth,  $\omega_{\mathbf{q}}$  is the lower polariton dispersion, and

$$\Gamma_{\mathbf{q},\text{TOT}} \equiv \Gamma_{\mathbf{q}}^{\text{pp}} + \Gamma_{\mathbf{q}}^{\text{ph}}, \quad (1c)$$

$$\Gamma_{\mathbf{q}}^{\text{pp}} = 2 \sum_{\mathbf{k}, \mathbf{k}'} \text{Re} G_{(\mathbf{k}, \mathbf{k}', \mathbf{k} + \mathbf{k}' - \mathbf{q})} W_{\mathbf{k}, \mathbf{k}', \mathbf{q}}^2 (N_{\mathbf{k}} + 1)(N_{\mathbf{k}'} + 1)N_{\mathbf{k} + \mathbf{k}' - \mathbf{q}},$$

$$\Gamma_{\mathbf{q}}^{\text{ph}} = 2 \sum_{\mathbf{q}', \mathbf{k}} \text{Re} G_{(\mathbf{q}, \mathbf{q}', \mathbf{k})}^{\text{ph}} W_{\mathbf{q} \rightarrow \mathbf{q}', \mathbf{k}}^{\text{ph}} (N_{\mathbf{q}'} + 1),$$

$$\Delta_{\mathbf{q},\text{TOT}} \equiv \Delta_{\mathbf{q}}^{\text{pp}} + \Delta_{\mathbf{q}}^{\text{ph}}, \quad (1d)$$

$$\Delta_{\mathbf{q}}^{\text{pp}} = 2 \sum_{\mathbf{k}, \mathbf{k}'} \text{Re} G_{(\mathbf{k}, \mathbf{k}', \mathbf{k} + \mathbf{k}' - \mathbf{q})} W_{\mathbf{k}, \mathbf{k}', \mathbf{q}}^2 (N_{\mathbf{k}} + 1)(N_{\mathbf{k}'} + 1)N_{\mathbf{k} + \mathbf{k}' - \mathbf{q}},$$

$$\Delta_{\mathbf{q}}^{\text{ph}} = 2 \sum_{\mathbf{q}', \mathbf{k}} \text{Re} G_{(\mathbf{q}, \mathbf{q}', \mathbf{k})}^{\text{ph}} W_{\mathbf{q}' \rightarrow \mathbf{q}, \mathbf{k}}^{\text{ph}} N_{\mathbf{q}'},$$

$$G_{(\mathbf{k}, \mathbf{k}', \mathbf{k} + \mathbf{k}' - \mathbf{q})} = \frac{i\hbar(\omega_{\mathbf{q}} + \omega_{\mathbf{k} + \mathbf{k}' - \mathbf{q}} - \omega_{\mathbf{k}} - \omega_{\mathbf{k}'}) + (\gamma_{\mathbf{q}} + \gamma_{\mathbf{k} + \mathbf{k}' - \mathbf{q}} + \gamma_{\mathbf{k}} + \gamma_{\mathbf{k}'})}{\hbar^2(\omega_{\mathbf{q}} + \omega_{\mathbf{k} + \mathbf{k}' - \mathbf{q}} - \omega_{\mathbf{k}} - \omega_{\mathbf{k}'})^2 + (\gamma_{\mathbf{q}} + \gamma_{\mathbf{k} + \mathbf{k}' - \mathbf{q}} + \gamma_{\mathbf{k}} + \gamma_{\mathbf{k}'})^2},$$

$$G_{(\mathbf{q}, \mathbf{q}', \mathbf{k})}^{\text{ph}} = \frac{i(E_{\mathbf{k}}^{\text{ph}} - |\hbar\omega_{\mathbf{q}} - \hbar\omega_{\mathbf{q}'}|) + (\gamma_{\mathbf{q}} + \gamma_{\mathbf{q}'})}{(E_{\mathbf{k}}^{\text{ph}} - |\hbar\omega_{\mathbf{q}} - \hbar\omega_{\mathbf{q}'}|)^2 + (\gamma_{\mathbf{q}} + \gamma_{\mathbf{q}'})^2}.$$

The polariton-polariton scattering rates  $W_{\mathbf{k}, \mathbf{k}', \mathbf{q}}$  are defined in Ref. 8 while the expression of the relaxation rates due to the polariton-phonon scattering is<sup>9</sup>

$$\begin{aligned} W_{\mathbf{q} \rightarrow \mathbf{q}', \mathbf{k}}^{\text{ph}} = & \frac{2\pi}{\hbar} \delta_{\mathbf{q} - \mathbf{q}' - \mathbf{k}} |X_{\mathbf{q}'}^* \langle \mathbf{q}' | \langle 0_{\mathbf{k}} | H_{\text{exc-ph}} | 1_{\mathbf{k}} \rangle \mathbf{q} \rangle X_{\mathbf{q}}|^2 [n_B(E_{\mathbf{k}}^{\text{ph}}) \\ & + \theta(\omega_{\mathbf{q}} - \omega_{\mathbf{q}'})], \end{aligned}$$

where  $H_{\text{exc-ph}}$  is the deformation-potential interaction,  $|n_{\mathbf{k}}\rangle$  is a phonon number state,  $|\mathbf{q}\rangle$  is the exciton state of wave vector  $\mathbf{q}$ ,  $X_{\mathbf{q}}$  is the exciton Hopfield coefficient,  $E_{\mathbf{k}}^{\text{ph}}$  is the energy of a phonon with wave vector  $\mathbf{k}$ ,  $n_B(E)$  is the Bose occupation, and  $\theta(w)$  is the Heaviside function. Notice that, here, the sums span over the whole lower polariton branch. Equations (1a)–(1d) are valid for all values of  $\mathbf{q}$  and account for the pump mechanism and for the polariton-phonon scattering,<sup>9</sup> which is considered in the Markov approximation, and is responsible for the relaxation into the lower polariton states. In particular, contrary to the reservoir-based approach, in the mean-field approach we can explicitly distinguish between the contributions due to the scattering processes internal to the polariton system and those due to the interaction with the phonon bath. The incoherent continuous pump is modeled by a source term entering in the equations for the populations  $N_{\mathbf{q}}$  and having a Gaussian weight

$$F_{\mathbf{q}} = F_0 \exp[-(E_{\mathbf{q}} - E_P)^2 / \sigma^2]. \quad (2)$$

In Eq. (2)  $E_{\mathbf{q}} = \hbar\omega_{\mathbf{q}}$  and  $E_P$  are the energy of the lower polariton mode and the pump energy, respectively. We have checked that the results do not depend on the specific values of the parameters  $E_P$  and  $\sigma$ , provided that the energy  $E_P$  be much larger than the exciton energy and  $\sigma$  be sufficiently small to avoid direct pumping into the bottom of the dispersion. This is a consequence of the long radiative lifetime of the excitons, which makes a quasithermalization possible within the high-energy region. These mechanisms are essential in order to describe the formation of a polariton population in the modes with small values of  $\mathbf{q}$ . In the mean-field approach, we account for the phonon-mediated scattering processes along the whole lower polariton branch. This produces an additional difference with respect to Ref. 8 where these processes are not considered. It is therefore interesting to investigate the importance of phonon scattering in determining the influence of noise. This is discussed in Fig. 2, where we compare the contributions with the effective gain,  $\Delta_{0,\text{TOT}} - \Gamma_{0,\text{TOT}}$ , due to the coupling to the phonon bath and to the internal scattering processes. With the system parameters used here, the phonon contribution does not exceed the 10% of the total gain. This indicates that the contribution to the noise in both models is essentially determined by the polariton-polariton scattering.

The master equation introduced in Ref. 8 allows evaluating the statistics of the polariton condensate and its solution is used in order to calculate the second-order correlation function in both schemes. The results are presented in Fig. 3.

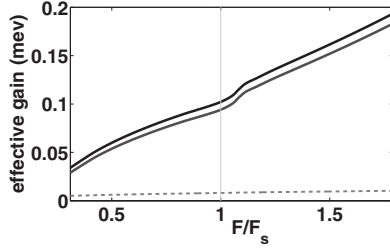


FIG. 2. Plot of the gain in the mean-field model as a function of the normalized pump intensity. The radiative lost ( $\gamma_0=0.1$  meV) is not included. Black curve: total effective gain  $\Delta_{0,\text{TOT}}-\Gamma_{0,\text{TOT}}$ . Gray curve: contribution of the polariton-polariton scattering. Dotted gray curve: contribution of the polariton-phonon scattering.  $F_s$  is the threshold intensity.

Both approaches show a deviation from the fully coherent behavior. This deviation is a consequence of the noise originating from the nonresonant scattering effects as already pointed out in Ref. 8. More important in the present context are the quantitative differences that exist between the results of the reservoir-based approach and those of the mean-field

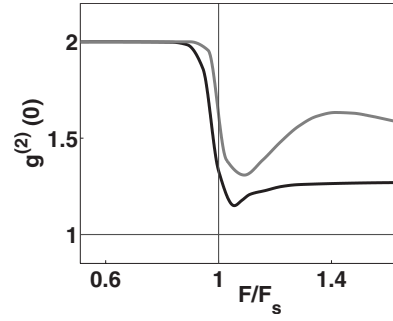


FIG. 3. Plot of the second-order correlation function as a function of the normalized pump intensity. Black curve: mean-field model. Gray curve: reservoir-based model.  $F_s$  is the threshold intensity.

approach. From the curves in Fig. 3 we infer that the reservoir-based approach overestimates the contribution of the scattering processes. The origin of this difference is understood from the equation describing the time evolution of the second-order correlation at equal times<sup>8</sup>

$$\begin{aligned} \hbar \frac{d}{d\tau} \langle P_0^+ P_0^+ P_0 P_0 \rangle &= \langle P_0^+ P_0^+ P_0 P_0 \rangle - \frac{(\Gamma_{11} - \Delta_{11})}{(6\Delta_{11} + \Delta_{0,\text{TOT}} - (\Gamma_{11} + \Gamma_{0,\text{TOT}}) - \gamma_0)} \langle P_0^+ P_0^3 \rangle + \frac{(16\Delta_{11} + 2\Delta_{0,\text{TOT}})}{(6\Delta_{11} + \Delta_{0,\text{TOT}} - (\Gamma_{11} + \Gamma_{0,\text{TOT}}) - \gamma_0)} \langle P_0^+ P_0 \rangle \\ &+ \frac{2\Delta_{11}}{(6\Delta_{11} + \Delta_{0,\text{TOT}} - (\Gamma_{11} + \Gamma_{0,\text{TOT}}) - \gamma_0)}. \end{aligned} \quad (3)$$

In the above equation we have introduced the dimensionless time  $\tau = [6\Delta_{11} + \Delta_{0,\text{TOT}} - (\Gamma_{11} + \Gamma_{0,\text{TOT}}) - \gamma_0]t$ , where  $6\Delta_{11} + \Delta_{0,\text{TOT}} - (\Gamma_{11} + \Gamma_{0,\text{TOT}}) - \gamma_0$  represents the gain. The quantity  $\gamma_0$  represents the cavity losses. The quantities  $\Gamma_{11}$  and  $\Delta_{11}$  originate in processes in which a polariton pair is subtracted from or injected into the mode with  $q=0$ , respectively, due to the exchange of two polaritons with opposite wave vector. The quantities  $\Delta_{0,\text{TOT}}$  and  $\Gamma_{0,\text{TOT}}$  describe the subtraction and injection of one polariton into the mode  $q=0$ , respectively. These quantities originate either in the interaction with the reservoir or in the resonant scattering between the modes with  $\mathbf{q} \neq 0$ . The detailed definition of all coefficients in the reservoir-based approach is given in Ref. 8. On the other hand, in the mean-field approach,

$$\Gamma_{11} = 2 \sum_{\mathbf{q}} G_{\mathbf{q}}^r W_{0,\mathbf{q},-\mathbf{q}}^2 (N_{\mathbf{q}} + 1)(N_{-\mathbf{q}} + 1), \quad (4a)$$

$$\Delta_{11} = 2 \sum_{\mathbf{q}} G_{\mathbf{q}}^r W_{0,\mathbf{q},-\mathbf{q}}^2 N_{\mathbf{q}} N_{-\mathbf{q}}, \quad (4b)$$

and

$$G_{\mathbf{q}}^r = \text{Re} \left\{ \frac{1}{i\hbar(\omega_{\mathbf{q}} - \omega_0) + \gamma_{\mathbf{q}} + \gamma_0} \right\}. \quad (4c)$$

The inhomogeneous term in Eq. (3) that describes the effects of noise on the second-order correlation of the condensate consists in the ratio between the nonresonant injection rate and the gain. This ratio determines the stationary behavior of the second-order correlation. Therefore, comparing the behavior of this quantity in both approaches, we obtain a picture of the relative relevance of the noise effects. This comparison in function of the normalized pump intensity is presented in Fig. 4.

The results presented in Fig. 4 confirm the fact that the noise effects are overestimated in the reservoir-based approach. In fact the noise-gain ratio strongly grows above threshold while in the mean-field approach this same ratio rapidly saturates. Therefore, the influence of noise on the second-order correlation in the mean-field approach is smaller than the one found in the reservoir-based approach. The main reason for this behavior lays in the different relevance of the gain in both approaches. As shown in Fig. 2 the effective gain in the mean-field model increases strongly and almost linearly. On the contrary, in the reservoir-based model the growth rate of the gain turns out to be extremely small (not shown here). This behavior explains the trend of the noise over gain ratio presented in Fig. 4. Notice that the

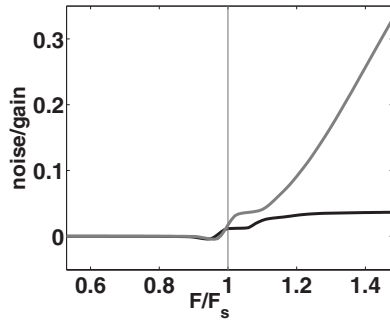


FIG. 4. Plot of the ratio of the noise over the gain as a function of the normalized pump intensity. Black curve: mean-field model. Gray curve: reservoir-based model.  $F_s$  is the threshold intensity.

quantities entering in the definition of the gain depend on the polariton population  $N_q$ . Therefore, in order to understand the different growth rates of the gain we have to discuss the behavior of the population in both models. In Fig. 5 we compare the population  $n(E)$  obtained within the two approaches for a pump value  $F=1.2 F_s$ , where the actual threshold value depends on the model considered. The two distributions differ significantly both in the very low-energy region and in their high-energy tail shown in the inset. In the low-energy region, the reservoir-based approach predicts a narrow distribution, with a large occupation of the ground state and of the first excited states (within an interval of 0.1 meV), while the mean-field approach results in a much more broadened distribution, with a large occupation of the excited states up to 1 meV above the ground state. This difference explains why, just above the threshold, the reservoir-based approach overestimates the weight of noise with respect to the mean-field approach. In fact, in the reservoir-based approach, the growth rate of the effective gain  $\Delta_{0,\text{TOT}} - \Gamma_{0,\text{TOT}}$  is small because of the relative small occupation of the states. On the contrary, the growth rate of the noise is large due to the large occupation at very low energy. In the mean-field approach, due to the broadened distribution, the growth rate of the gain is large and compensates the increase in the noise. A different behavior between the two models is also found at very high energy, where the reservoir-based ap-

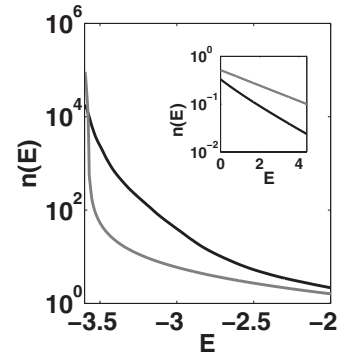


FIG. 5. Plot of the polariton occupation number  $n(E)$  as a function of the energy. Black curve: mean-field model. Gray curve: reservoir-based model. The pump intensity is  $F/F_s=1.2$ . The inset presents the same plot for larger positive energies.

proach predicts a much larger effective temperature. In fact, while in the mean-field approach, the population tends to equilibrium as a whole, in the reservoir-based approach, an artificial separation is introduced between active and reservoir polaritons leading to a separate approach to equilibrium of both components.

In conclusion, the result presented in Fig. 3 confirms that the deviation from full coherence in the second-order correlation function of the condensate observed in the experiments is qualitatively reproduced in the master-equation approach. This result is independent on the model chosen in order to describe the population dynamics. It also confirms that the deviation from full second-order coherence is mainly due to the nonresonant scattering processes between polariton pairs. The two approaches lead to quantitatively different results when comparing the noise effects. These differences are related to the different modeling of the dynamics of the polariton populations in the high-energy region of the polariton dispersion. The present results show that in the reservoir-based approach the effects of noise are overestimated with respect to the ones calculated in the mean-field approach. This fact is related to the assumption of a reservoir for the bottleneck polaritons that leads to an abrupt thermalization of the polaritons at high energy.

<sup>1</sup>J. Kasprzak, M. Richard, S. Kundermann, A. Baas, P. Jeambrun, J. M. J. Keeling, F. M. Marchetti, M. H. Szymanska, R. Andre, J. L. Staehli, V. Savona, P. B. Littlewood, B. Deveaud, and L. S. Dang, *Nature* (London) **443**, 409 (2006).

<sup>2</sup>R. Balili, V. Hartwell, D. Snoke, L. Pfeiffer, and K. West, *Science* **316**, 1007 (2007).

<sup>3</sup>H. Deng, G. S. Solomon, R. Hey, K. H. Ploog, and Y. Yamamoto, *Phys. Rev. Lett.* **99**, 126403 (2007).

<sup>4</sup>S. Christopoulos, G. Baldassarri Hoyer von Hogerthal, A. Grundy, P. G. Lagoudakis, A. V. Kavokin, J. J. Baumberg, G. Christmann, R. Butte, E. Feltn, J. F. Carlin, and N. Grandjean, *Phys. Rev. Lett.* **98**, 126405 (2007).

<sup>5</sup>J. Kasprzak, M. Richard, A. Baas, B. Deveaud, R. Andre, J. P. Poizat, and L. S. Dang, *Phys. Rev. Lett.* **100**, 067402 (2008).

<sup>6</sup>H. Deng, G. Weihs, C. Santori, J. Bloch, and Y. Yamamoto,

*Science* **298**, 199 (2002).

<sup>7</sup>G. Ruompos, C. W. Lai, A. Forchel, and Y. Yamamoto, March Meeting 2008 (American Physical Society, New York, 2008), Paper No. R100330.

<sup>8</sup>P. Schwendimann and A. Quattropani, *Phys. Rev. B* **77**, 085317 (2008).

<sup>9</sup>F. Tassone, C. Piermarocchi, V. Savona, A. Quattropani, and P. Schwendimann, *Phys. Rev. B* **56**, 7554 (1997).

<sup>10</sup>M. Sargent, M. O. Scully, and W. E. Lamb, *Laser Physics* (Addison-Wesley, London, 1974).

<sup>11</sup>D. Porras, C. Ciuti, J. J. Baumberg, and C. Tejedor, *Phys. Rev. B* **66**, 085304 (2002).

<sup>12</sup>F. Tassone and Y. Yamamoto, *Phys. Rev. B* **59**, 10830 (1999).

<sup>13</sup>T. D. Doan, H. T. Cao, D. B. Tran Thoai, and H. Haug, *Phys. Rev. B* **74**, 115316 (2006).